

CLINICAL AND POPULATION SCIENCES

Unique Subtype of Microglia in Degenerative Thalamus After Cortical Stroke

Zhijuan Cao¹ MD, PhD; Sean S. Harvey¹ BS; Terrance Chiang, BS; Aulden G. Foltz¹; Alex G. Lee, PhD; Michelle Y. Cheng¹ PhD*; Gary K. Steinberg¹ MD, PhD*

BACKGROUND AND PURPOSE: Stroke disrupts neuronal functions in both local and remotely connected regions, leading to network-wide deficits that can hinder recovery. The thalamus is particularly affected, with progressive development of neurodegeneration accompanied by inflammatory responses. However, the complexity of the involved inflammatory responses is poorly understood. Herein we investigated the spatiotemporal changes in the secondary degenerative thalamus after cortical stroke, using targeted transcriptome approach in conjunction with histology and flow cytometry.

METHODS: Cortical ischemic stroke was generated by permanent occlusion of the left middle cerebral artery in male C57BL/6J mice. Neurodegeneration, neuroinflammatory responses, and microglial activation were examined in naive and stroke mice at from poststroke days (PD) 1 to 84, in both ipsilesional somatosensory cortex and ipsilesional thalamus. NanoString neuropathology panel (780 genes) was used to examine transcriptome changes at PD7 and PD28. Fluorescence activated cell sorting was used to collect CD11c⁺ microglia from ipsilesional thalamus, and gene expressions were validated by quantitative real-time polymerase chain reaction.

RESULTS: Neurodegeneration in the thalamus was detected at PD7 and progressively worsened by PD28. This was accompanied by rapid microglial activation detected as early as PD1, which preceded the neurodegenerative changes. Transcriptome analysis showed higher number of differentially expressed genes in ipsilesional thalamus at PD28. Notably, neuroinflammation was the top activated pathway, and microglia was the most enriched cell type. *Itgax* (CD11c) was the most significantly increased gene, and its expression was highly detected in microglia. Flow-sorted CD11c⁺ microglia from degenerative thalamus indicated molecular signatures similar to neurodegenerative disease-associated microglia; these included downregulated *Tmem119* and *CX3CR1* and upregulated *ApoE*, *Axl*, *LpL*, *CSF1*, and *Cst7*.

CONCLUSIONS: Our findings demonstrate the dynamic changes of microglia after stroke and highlight the importance of investigating stroke network-wide deficits. Importantly, we report the existence of a unique subtype of microglia (CD11c⁺) with neurodegenerative disease-associated microglia features in the degenerative thalamus after stroke.

GRAPHIC ABSTRACT: An online [graphic abstract](#) is available for this article.

Key Words: cerebral ischemia ■ microglia ■ neuroinflammation ■ transcriptome

Stroke is a leading cause of long-term disability in the United States.¹ A stroke injury can disrupt neuronal function in both local and remotely connected regions, leading to network-wide deficits that can hinder recovery.² In particular, a delayed secondary injury

progressively develops in the remotely connected thalamus after the initial cortical stroke.^{3,4} The disruption of functional connections between cortex and thalamus causes cortical anterograde degeneration and thalamic retrograde degeneration, resulting in the secondary

Correspondence to: Gary K. Steinberg, MD, PhD, Department of Neurosurgery, Stanford University School of Medicine, 300 Pasteur Dr (R301A), Stanford, CA 94305, Email gsteinberg@stanford.edu or Michelle Y. Cheng, PhD, Department of Neurosurgery, Stanford University School of Medicine, 1201 Welch Rd, MSLS (P308), Stanford, CA 94305, Email mycheng@stanford.edu

*Drs Cheng and Steinberg contributed equally.

The Data Supplement is available with this article at <https://www.ahajournals.org/doi/suppl/10.1161/STROKEAHA.120.032402>.

For Sources of Funding and Disclosures, see page 697.

© 2021 American Heart Association, Inc.

Stroke is available at www.ahajournals.org/journal/str

Nonstandard Abbreviations and Acronyms

DAM	disease-associated microglia
DEG	differentially expressed gene
iS1	ipsilesional somatosensory cortex
iTH	ipsilesional thalamus
PD	poststroke day

thalamic injury (Figure 1A).⁵ Secondary thalamic injury has been reported in a subset of stroke patients with cortical stroke. This delayed secondary injury has been associated with long-term functional deficits, including verticality misperception, lower verbal fluency performance and poor motor, cognitive and emotional outcome after stroke.^{6,7} Rodent studies have shown that reducing secondary thalamic injury is beneficial for long-term behavioral recovery.^{8,9} Hence, targeting secondary thalamic injury is a promising strategy to improve recovery after stroke. In addition, secondary thalamic injury is a delayed injury that progressively develops,^{3,4,7} thus allowing an extended time window for therapeutic intervention.

Emerging studies indicate multiple pathological changes occur in the secondary thalamic injury after stroke, including excitotoxicity,¹⁰ apoptosis,¹¹ amyloid protein deposition,¹² blood-brain-barrier breakdown,⁹ and neuroinflammation.¹³ There is a growing interest in the mechanisms of neuroinflammation in the secondary thalamic injury.¹⁴ Multiple cell types (resident microglia, astrocytes, and oligodendrocytes as well as peripheral T cells) and molecular mediators participate in neuroinflammation in the secondary thalamic injury.^{15–17} In animal models, markers of microglia/macrophages activation such as CD68, ionized calcium binding adapter molecule 1 (Iba-1), and marker of astrocyte activation GFAP (glial fibrillary acidic protein)^{8,18} are elevated in the connected thalamus at one month after cortical stroke. In patients, microglial/macrophage activations are detected in the thalamus between 2 and 24 months after initial cortical infarctions.¹⁷ However, the complexity of neuroinflammatory responses during the development of secondary thalamic injury is poorly understood, thus making it challenging to develop targeted immunomodulatory therapies to reduce this injury.

To investigate the spatiotemporal changes in thalamus after stroke, we conducted a long-term time course study to track the progressive development of neurodegeneration and neuroinflammation in a cortical stroke mouse model. Using a targeted neuropathology transcriptome analysis, we detected key cell types and molecular changes involved in both somatosensory cortex (the primary injury) and ipsilesional thalamus (iTH; the secondary injury) after stroke. Our findings identified a unique subtype of microglia with neurodegenerative disease-specific features in the degenerative thalamus after stroke. We also highlighted potential molecular

targets for intervening secondary thalamic injury to improve recovery after stroke.

METHODS

Below are the main methods necessary to comprehend the results. Please see materials and methods in the [Data Supplement](#) for details. Data supporting the findings of this study are available from the corresponding authors via written request.

Animals

Experiments were performed in adult C57BL/6J wild-type male mice (12–15 weeks old and 28–37 g body weight; The Jackson Laboratory, Bar Harbor, ME). We used only male mice to be consistent with our previous findings which were obtained in male mice. The effects of sex differences will be explored in future studies. Animals were housed under a 12-hour light-dark cycle with food and water provided *ad libitum*. All experiments were performed under the guidelines of Stanford University Institutional Animal Care and Use. A total of 123 mice were randomized and subjected to stroke group (108 mice) and naive group (15 mice). Naive mice were used as nonoperated controls. In stroke group, mice were subjected to permanent occlusion of left distal middle cerebral artery. Mortality rate was zero. Samples were collected at poststroke day (PD) 1, 3, 7, 14, 28, 56, and 84. In the final analysis, 18 mice were excluded in stroke group due to lack of primary infarction at somatosensory cortex evaluated by T2 magnetic resonance imaging or histology,¹⁹ and one mouse was excluded in naive group due to outlier in transcriptome analysis.

NanoString Transcriptome Analysis

For nCounter gene expression analysis, tissue samples were dissected from ipsilesional somatosensory cortex (iS1) and iTH in stroke mice and corresponding regions in naive mice. One hundred nanograms of total RNA from individual sample were used, and the assay was performed by Core Diagnostics, Inc (Hayward, CA) following the manufacturer's protocol. A total of 780 genes were analyzed including 770 genes from Neuropathology panels (XT-CSO-MNROP1-12, NanoString Technologies, Seattle, WA) and 10 spike in genes (CodeSet designed by NanoString as listed in Table I in the [Data Supplement](#)). These genes are involved in neurotransmission, neuron-glia interaction, neuroplasticity, cell structure integrity, neuroinflammation, and metabolism.

Fluorescence Activated Cell Sorting

iTH and contralesional thalamus samples were dissected from a subset of PD28 mice, and each sample was pooled from 8 mice. Naive samples were dissected at corresponding positions in naive mice. The isolated immune cells were incubated with Live/Death-Aqua stain then antibodies (CD45, CD11b, and CD11c, as listed in Table II in the [Data Supplement](#)). Forward and side scatter were used to gate singlet cell events. Aqua positive stained events were further excluded as collection of dead cells. Unstained cells were used to eliminate autofluorescence. Microglia (CD45^{int}CD11b⁺), CD11c⁺ microglia (CD45^{int}CD11

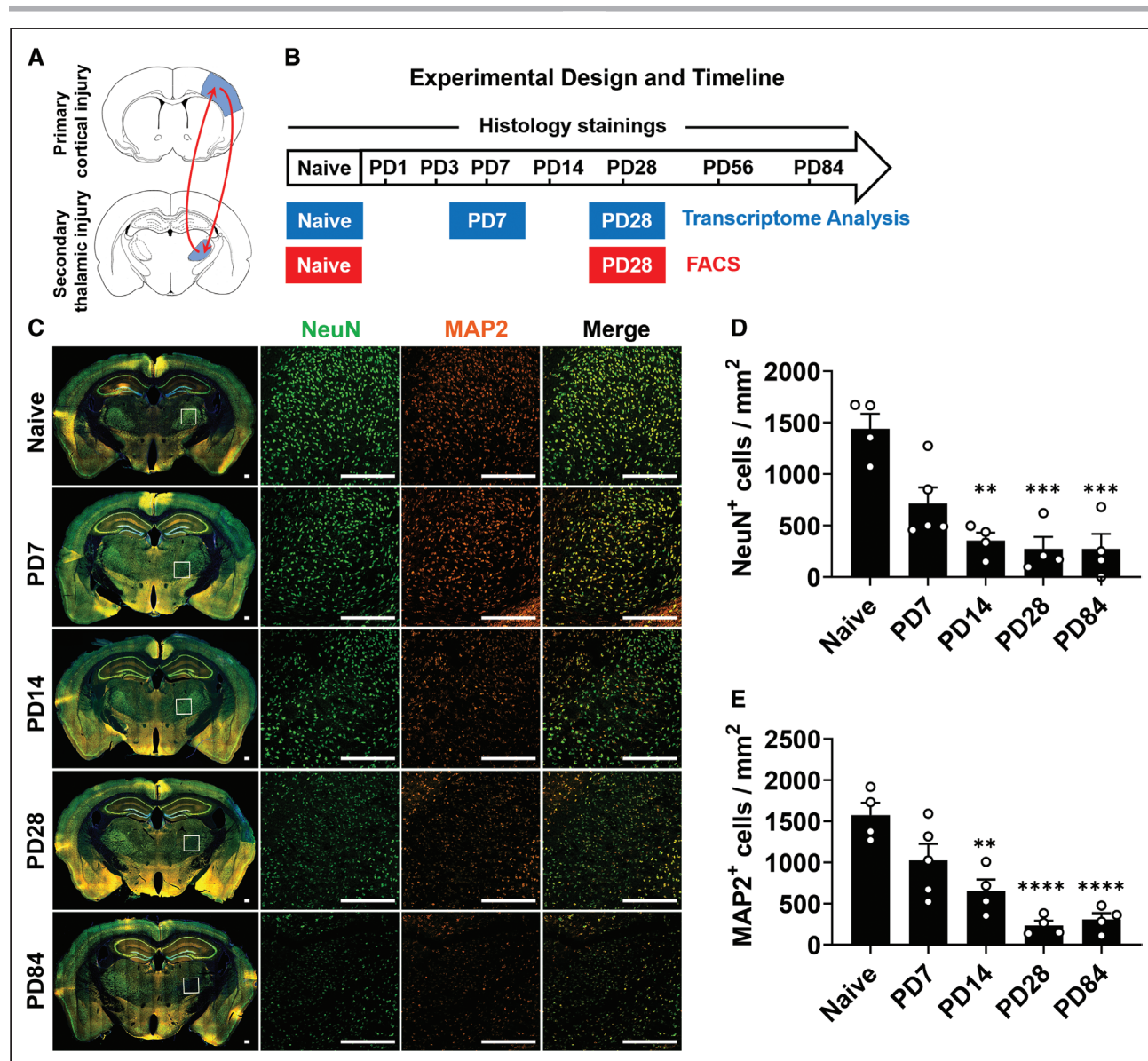


Figure 1. Delayed neuron loss in thalamus after primary cortical ischemic injury.

A, Diagram shows the location of secondary thalamic injury (blue labeled area in **bottom** section) after primary cortical injury (blue labeled area in **upper** section). The thalamic degeneration results in the anterograde/retrograde degeneration (arrows) after disruption of cortico-thalamic connections. **B**, Experimental design and timeline. A time course histology study was performed to detect spatiotemporal changes in somatosensory cortex and thalamus after stroke. Transcriptome analysis was performed on samples collected from naive, poststroke day (PD7; beginning of secondary thalamic injury), and PD28 (severe secondary thalamic injury). Fluorescence activated cell sorting (FACS) was used to sort microglia and CD11c⁺ microglia from naive and PD28 thalamic tissues respectively to detect molecular features of CD11c⁺ microglia. **C**, Representative full coronal sections show NeuN (green) and MAP2 (microtubule-associated protein 2; orange) immunostaining in thalamus. Enlarged images represent the square labeled region in full section images. Scale bar=250 μ m. The numbers of NeuN⁺ cell (**D**) and MAP2⁺ cell (**E**) in iTH were counted and compared with naive. N=4–5/time point. ** P <0.01, *** P <0.001, **** P <0.0001. Data are expressed as mean \pm SEM.

b⁺CD11c⁺), and CD11c⁻ microglia (CD45^{int}CD11b⁺CD11c⁻) were sorted by Sony SH800 (Stanford Shared Fluorescence Activated Cell Sorting Facility). The sorted cells were collected in 300 μ L QIAGEN RNA protect Cell Reagent (76526, QIAGEN) and stored in 4°C until RNA extraction.

Statistical Analysis

All data were expressed as mean \pm SEM and analyzed using GraphPad Prism (version 8.0.2, GraphPad Software, San Diego,

CA; www.graphpad.com). Shapiro-Wilk test was used to test for normal distribution. For histology studies, data were analyzed by either 1-way ANOVA (parametric) followed by Bonferroni test for multiple comparisons with naive control group or Kruskal-Wallis test (nonparametric) followed by Dunn test for multiple comparisons with naive control group. All other data were analyzed by 1-way ANOVA followed by multiple comparisons with every other groups by Bonferroni test. Significance level was set at P <0.05.

RESULTS

Secondary Thalamic Injury Progressively Developed After Primary Cortical Stroke

We first performed a histological time course study from PD1 to PD84, which includes both the acute and the long-term phases after stroke (see experimental timeline and design in Figure 1B). Degeneration was detected by Fluoro-Jade C staining. In iS1, Fluoro-Jade C-labeled cell bodies were observed as early as PD1 and remained detectable until PD84 (Figure 1A in the [Data Supplement](#)). In iTH, the area of Fluoro-Jade C positively stained was significantly increased from PD7 to PD28, and the intensity of Fluoro-Jade C was significantly increased from PD7 up to PD84 (Figure 1B through 1D in the [Data Supplement](#)). Neuronal loss was visualized by NeuN and MAP2 (microtubule-associated protein 2). In iS1, weak NeuN was observed at PD1 and PD3 and barely seen after PD7 up to PD84 in the infarct core (Figure 1E in the [Data Supplement](#)). As early as PD1 and continuously up to PD84, no MAP2 staining was observed in infarct core. In peri-infarct areas (Figure 1E in the [Data Supplement](#) enlarged images), NeuN remained evident at PD1 and PD3 but continued to decrease after PD3, whereas intense MAP2 was expressed around the border of infarct from PD1 up to PD84. These data confirmed a primary neuronal loss in iS1. In iTH, the numbers of NeuN⁺ and MAP2⁺ cells began to decrease at PD7, with significant reductions at PD14 and PD28 (Figure 1C through 1E). By PD84, numbers of NeuN⁺ cells decreased 81.0% and numbers of MAP2⁺ cells decreased 80.5%, indicating delayed neuron loss in iTH. Taken together, these findings indicated that secondary thalamic neurodegeneration began at PD7 and progressively developed through PD84 in our cortical stroke mouse model.

Neuropathological Transcriptome Analysis of Primary Cortical Injury and Secondary Thalamic Injury After Stroke

To profile the molecular changes after stroke, we performed a targeted neuropathological transcriptome analysis. Hierarchical clustering analysis showed distinct cluster separation between naïve and PD7 in iS1, except one PD7 sample clustered with naïve samples, possibly due to variability in cerebral infarct size (Figure 2A). In contrast, clear cluster separation was shown in iS1 at PD28, suggesting the consistent long-term effects in the primary cortical injury. In iTH, clear cluster separations were shown at PD7 and PD28 compared with naïve, revealing a consistent secondary thalamic injury after stroke. Supervised PCA plots showed similar results (Figure 2B in the [Data Supplement](#)). Differential transcriptome changes were detected in iS1 and iTH (Figure 2B and 2C). In iS1, transcriptome analysis revealed 294 differentially expressed genes (DEGs)

at PD7 (209 upregulated and 85 downregulated) and 38 DEGs at PD28 (12 upregulated and 26 downregulated; Tables III and IV in the [Data Supplement](#)). In contrast, iTH showed 50 DEGs at PD7 (44 upregulated and 6 downregulated) and 187 DEGs at PD28 (84 upregulated and 103 downregulated; Tables V and VI in the [Data Supplement](#)). Comparative analysis showed 26 common DEGs in iS1 and 37 common DEGs in iTH between PD7 and PD28 (Figure 2D). In iS1, 4 out of 26 common DEGs showed >2-fold changes, including *C3*, *GFAP*, *CD14*, and *Itgax*. In iTH, 15 out of 37 common DEGs showed >2-fold changes. Among these 15 genes, 13 of them are highly expressed in microglia as referred by the Brain RNA seq database (<http://www.brainrnaseq.org/>),²⁴ including *CD14*, *Ccl12*, *Slc11a1*, *TLR2*, *Fcrls*, *CD86*, *Cxcl16*, *Irf8*, *Cd68*, *C1qa*, *Trem2*, *C1qc*, and *C1qb*. Further cell type enrichment analysis also showed that more DEGs are enriched in microglia at both time points in iS1 and iTH (Figure 2E and Figure III B in the [Data Supplement](#)), indicating microglia as the top cell type activated after stroke and their critical involvement during the development of secondary thalamic injury.

Neuroinflammation Identified as the Top Canonical Pathway in Primary Cortical Injury and Secondary Thalamic Injury After Stroke

Next, we performed Ingenuity Pathway Analysis to identify the top-ranked diseases, cellular and molecular functions (Figure 3A) and canonical pathways (Figure 3B). Neuroinflammation was the top-ranked pathway activated in both iS1 and iTH at both PD7 and PD28. Other canonical pathway in iS1 includes Huntington's disease, endothelin-1, interleukin (IL)-8, and opioid signaling at PD7 and Huntington's disease, nuclear factor erythroid 2-related factor 2-mediated oxidative stress response, IL-8 and androgen signaling at PD28. Other canonical pathway in iTH includes wingless-related integration site/ β -catenin, dendritic cell maturation, role of pattern recognition receptors in recognition of bacteria and viruses and IL-12 signaling and production in macrophages at PD7, and production of nitric oxide and reactive oxygen species in macrophages, nuclear factor kappa B, and glucocorticoid receptor signaling at PD28. Using quantitative real-time polymerase chain reaction, we successfully validated several key genes expression in the neuroinflammation signaling pathway in iTH at PD28, including CSF1, CSF1R, CX3CR1, TGF β , TLR2, and TREM2 (Figure 3C and Figure III C in the [Data Supplement](#)).

Neuroinflammation in the Thalamus During the Development of Secondary Thalamic Injury After Cortical Stroke

We then used CD68 to detect microglia/macrophage activation and GFAP to detect astrocytes activation. In

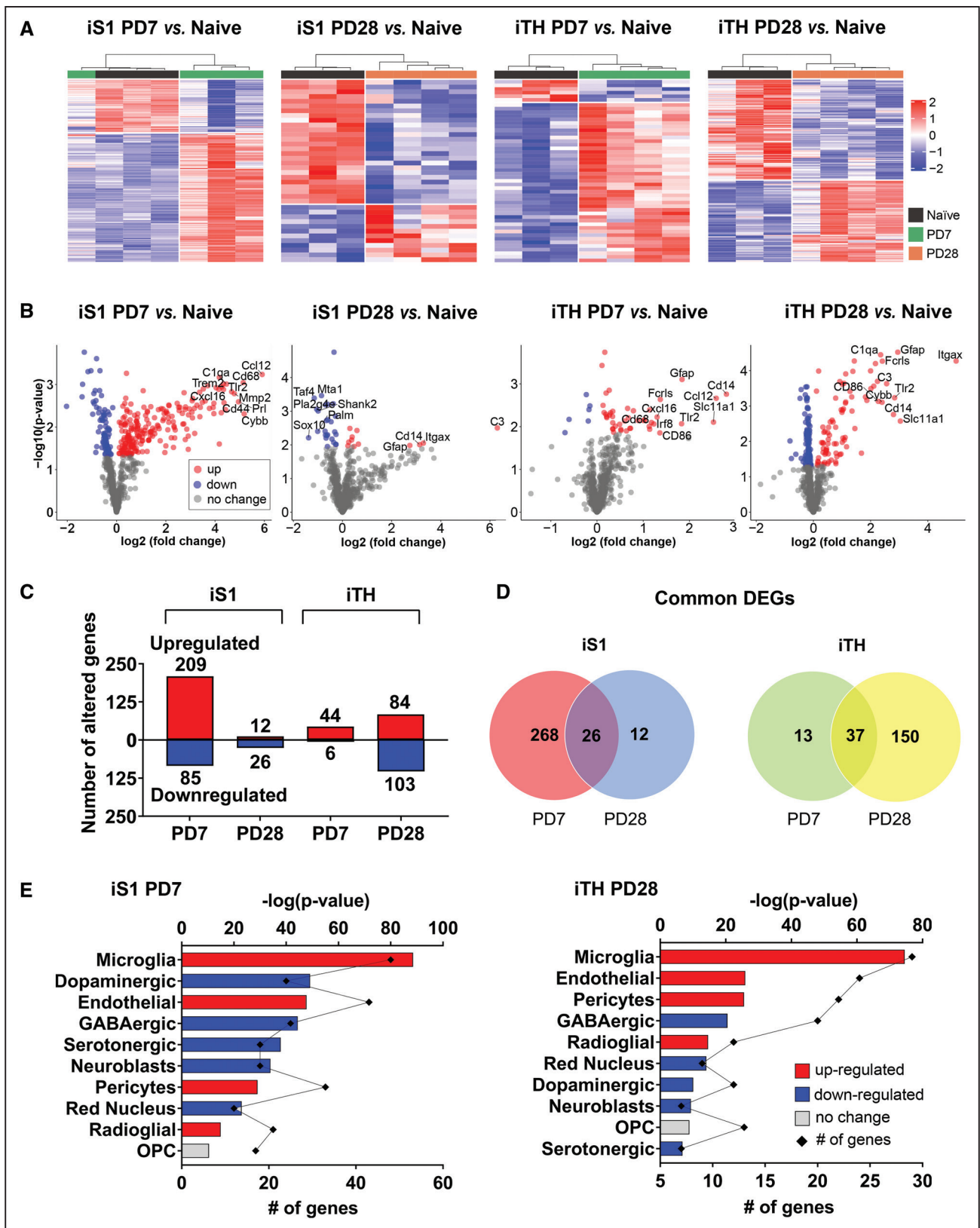


Figure 2. Targeted transcriptome analysis of somatosensory cortex and thalamus after cortical ischemic stroke. **A**, Heat map of differentially expressed genes (DEGs) in ipsilesional somatosensory cortex (iS1) and ipsilesional thalamus (iTH) at poststroke day (PD7) and PD28. **B**, Volcano plots show fold-change relative to naïve samples. Red, blue, and gray dots indicate upregulated, downregulated, and unchanged genes, respectively. Top 10 DEGs are labeled. N=3 in naïve, N=4 in PD7, and N=4 in PD28. **C**, Numbers of altered genes in iS1 and iTH (**D**) Venn diagram represents the number of common DEGs at 2 time points in iS1 and iTH. **E**, Bar graphs indicate enriched cell types of DEGs in iS1 at PD7 and in iTH at PD28, plotted with $-\log_{10}(P \text{ value})$ and number of genes in the cell type. OPC indicates oligodendrocyte progenitor cell.

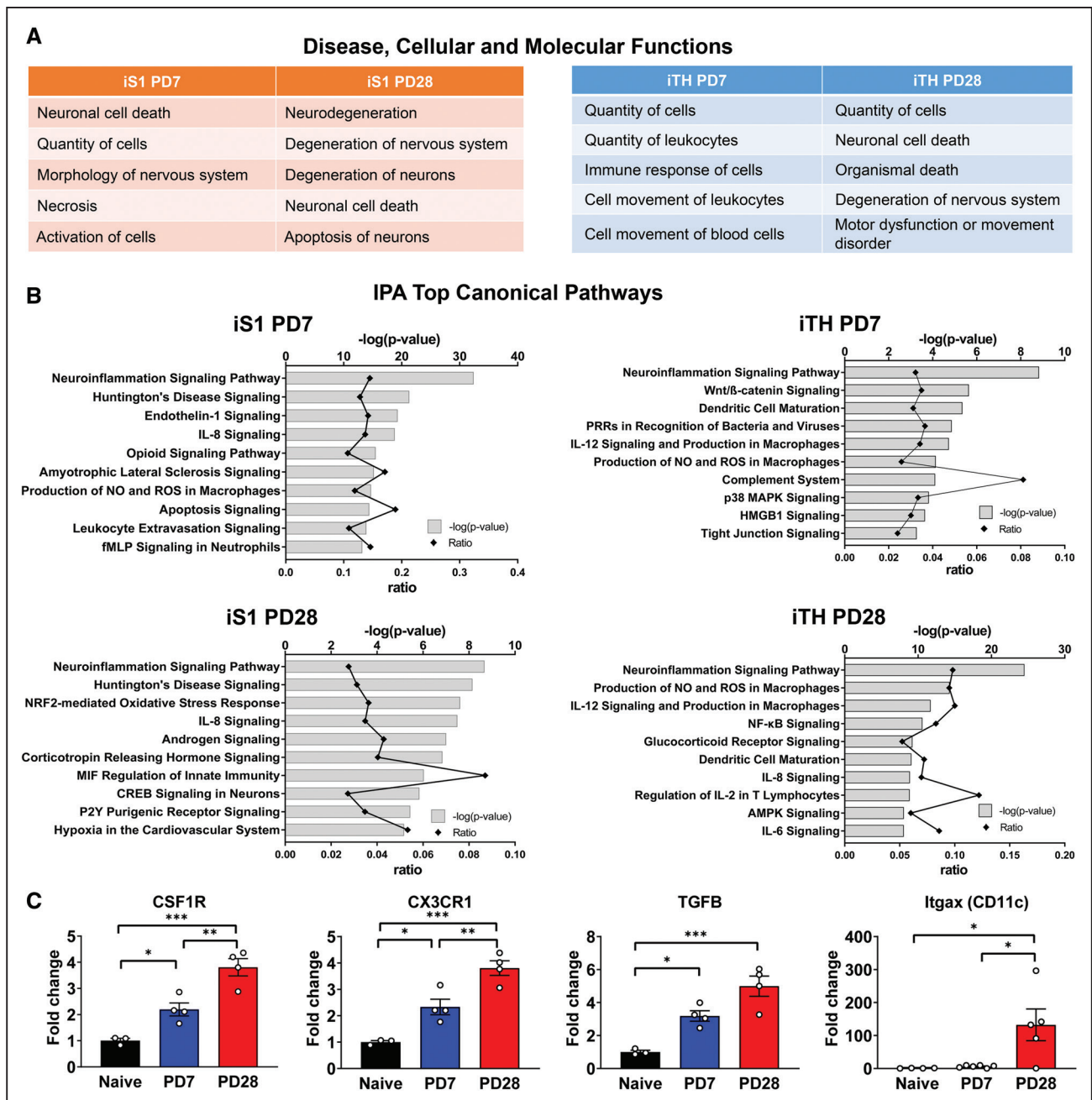


Figure 3. Ingenuity pathway analysis (IPA) highlighted the involvement of neuroinflammation signaling after stroke.

A, Top-ranked diseases and molecular/cellular functions. **B**, Top significant canonical pathways, plotted by $-\log_{10}(P \text{ value})$ and ratio. **C**, quantitative real-time polymerase chain reaction (qPCR) validated differentially expressed genes (DEGs) in neuroinflammation signaling (CSF1R, CX3CR1, and TGFB) in ipsilesional thalamus (iTH). N=3 in naive, N=4 in poststroke day (PD7), and N=4 in PD28. Itgax in iTH was quantified with another cohort of samples. N=4 in naive, N=6 in PD7, and N=5 in PD28. * $P < 0.05$, ** $P < 0.01$, *** $P < 0.001$. Data are expressed as mean \pm SEM. AMPK indicates AMP-activated protein kinase; CSF1R, colony stimulating factor 1 receptor; CREB, cAMP response element-binding protein; HMGB1, high mobility group box 1; IL, interleukin; iS1, ipsilesional somatosensory cortex; MAPK, mitogen-activated protein kinase; MIF, macrophage migration inhibitory factor; NF- κ B, nuclear factor kappa B; NO, nitric oxide; NRF2, nuclear factor erythroid 2-related factor 2; PRRs, pattern recognition receptors; ROS, reactive oxygen species; and TGFB, transforming growth factor beta.

iS1 (Figure IVA in the [Data Supplement](#)), CD68 was initially identified at peri-infarct areas at PD1 and gradually appeared in the infarct core at PD14. GFAP appeared sparsely around the infarct at PD3 and became densely packed and elongated at PD7, suggesting robust neuroinflammatory responses in iS1 after stroke. In iTH (Figure

IVB through IVD in the [Data Supplement](#)), CD68 was barely detectable at PD1 and GFAP was barely detectable before PD3. Compared with naive, CD68 and GFAP significantly increased at PD14, peaked at PD28 and greatly reduced at PD84 in the secondary thalamic injured area. Clustered CD68/GFAP staining was observed at PD14

and became denser at PD28. These data exhibited differential timing of neuroinflammatory responses between primary and secondary injuries after stroke.

Microglia Exhibited Dynamic Changes in Gene Expression and Morphology in the Thalamus After Cortical Stroke

We further used Tmem119 (transmembrane protein 119), a specific marker highly expressed on homeostasis microglia to detect microglia changes.²⁵ Iba-1 co-staining was used to visualize microglial/macrophage morphology. Tmem119 reduced in the infarct core in iS1 as early as PD1 and continuously decreased up to PD28 (Figure V in the [Data Supplement](#)). After PD56, a few Tmem119⁺ cells with round shape morphology were observed in the infarct core. In peri-infarct areas, Tmem119 reduced from PD1 to PD28, but returned to similar levels as naïve at PD56 and PD84. In iS1, Iba-1 was detected at peri-infarct areas from PD1 to PD7 and robustly shown in the infarct core after PD7 (Figure V in the [Data Supplement](#)). These findings suggested a dynamic microglia/macrophage activation in the primary cortical injury after stroke. In iTH, Tmem119⁺ microglia showed morphological changes as early as PD1 (Figure 4A), suggesting the rapid microglia response in remote iTH after primary cortical stroke. Interestingly, Tmem119 intensity progressively decreased after PD7 and was low to undetectable between PD14 and PD84 (Figure 4A and 4B). In contrast, Iba-1 was low in PD1 but robustly increased after PD7, peaked at PD28, and decreased at PD84 (Figure 4A and 4C). These findings raised the question of whether these Tmem119^{low}Iba-1⁺ cells in the degenerative thalamus are activated microglia or macrophages. To address this, we used multi-color flow cytometry to quantify the myeloid cell types in iS1 and iTH at PD28 (Figure VIA in the [Data Supplement](#)). In iS1, 67.1±6.7% of total leukocytes were microglia (CD45^{int}CD11b⁺Ly6C⁻Ly6G⁻) and 5.0±0.7% were macrophages (CD45^{high}CD11b⁺). In iTH, 78.8±0.4% of total leukocytes were microglia and 1.4±0.8% were macrophages (Figure VIB and VIC in the [Data Supplement](#)). These data showed that more peripheral macrophages infiltrated into the primary cortical injury, while most of the myeloid cells remained as microglia in the secondary thalamic injury.

In addition, reconstructed 3-dimensional images showed the morphological changes of Iba-1⁺ cells in thalamus, from resting status in naïve to hyper-ramified at PD7, then transitioned to bushy/amoeboid at PD28 (Figure 4D). At PD84, Iba-1⁺ cells returned to resting/ramified status. These data suggest the dynamic change of microglia in gene expression and morphology during the development of secondary thalamic injury.

A Unique Subtype of Microglia Was Identified in Secondary Thalamic Injury After Cortical Stroke

To further hone in on key genes in iTH, we focused on the top significantly increased gene *Itgax* (Figure 2B). Using another cohort of samples, we validated the significant increase of *Itgax* in iTH at PD28 (Figure 3C). *Itgax*, codes for CD11c, a type I transmembrane protein expressed on dendritic cells but also found in other immune cells including microglia and macrophages.²⁶ On the time course brain sections (Figure 5A through 5C), CD11c was absent at naïve, PD1, PD3, and barely detectable at PD7 in the thalamus. Interestingly, prominent CD11c was detected at PD14, robustly increased at PD28 and dropped to basal levels after PD56 in iTH. At PD28, CD11c co-expressed in 82.0±3.6% Iba-1⁺ cells. These data suggest a subpopulation of microglia (CD11c⁺) in the degenerative thalamus after stroke.

CD11c⁺ Microglia in Degenerative Thalamus Exhibited Molecular Signatures of Neurodegenerative Disease-Associated Microglia

Recently a novel subtype of microglia, disease-associated microglia (DAM), was identified in neurodegenerative disease models.²⁶ All DAM were reported to express CD11c.²⁶ Next, we sorted CD11c⁺ microglia from iTH at PD28 (Figure 6A) and detected expression of a set of representative genes of DAM on them. Consistent with our immunostaining result, CD11c⁺ microglia presented specifically in iTH at PD28 but not in naïve and contralesional thalamus (Figure 6B). *Itgax* abundantly expressed on the sorted iTH CD11c⁺ cells (Figure 6C). Compared with iTH CD11c⁻, contralesional thalamus and naïve microglia (CD45^{int}CD11b⁺), Tmem119, and CX3CR1 were significantly decreased, while ApoE, Axl, LpL, CSF1, and Cst7 genes were significantly increased in iTH CD11c⁺ microglia, suggesting molecular signatures of CD11c⁺ microglia in iTH at PD28 are similar as DAM (Figure 6D).

DISCUSSION

To the best of our knowledge, this is the first comprehensive spatiotemporal study that demonstrates dynamic microglia activation in the remotely connected thalamus after cortical stroke. Our time course histological data showed progressive neuronal loss accompanied by robust neuroinflammation in the thalamus after stroke. Transcriptome analysis revealed neuroinflammation as the top signaling pathway and microglia as the key cell type during the development of secondary thalamic injury. Microglia exhibited rapid and dynamic changes in morphology and gene expression in the degenerative

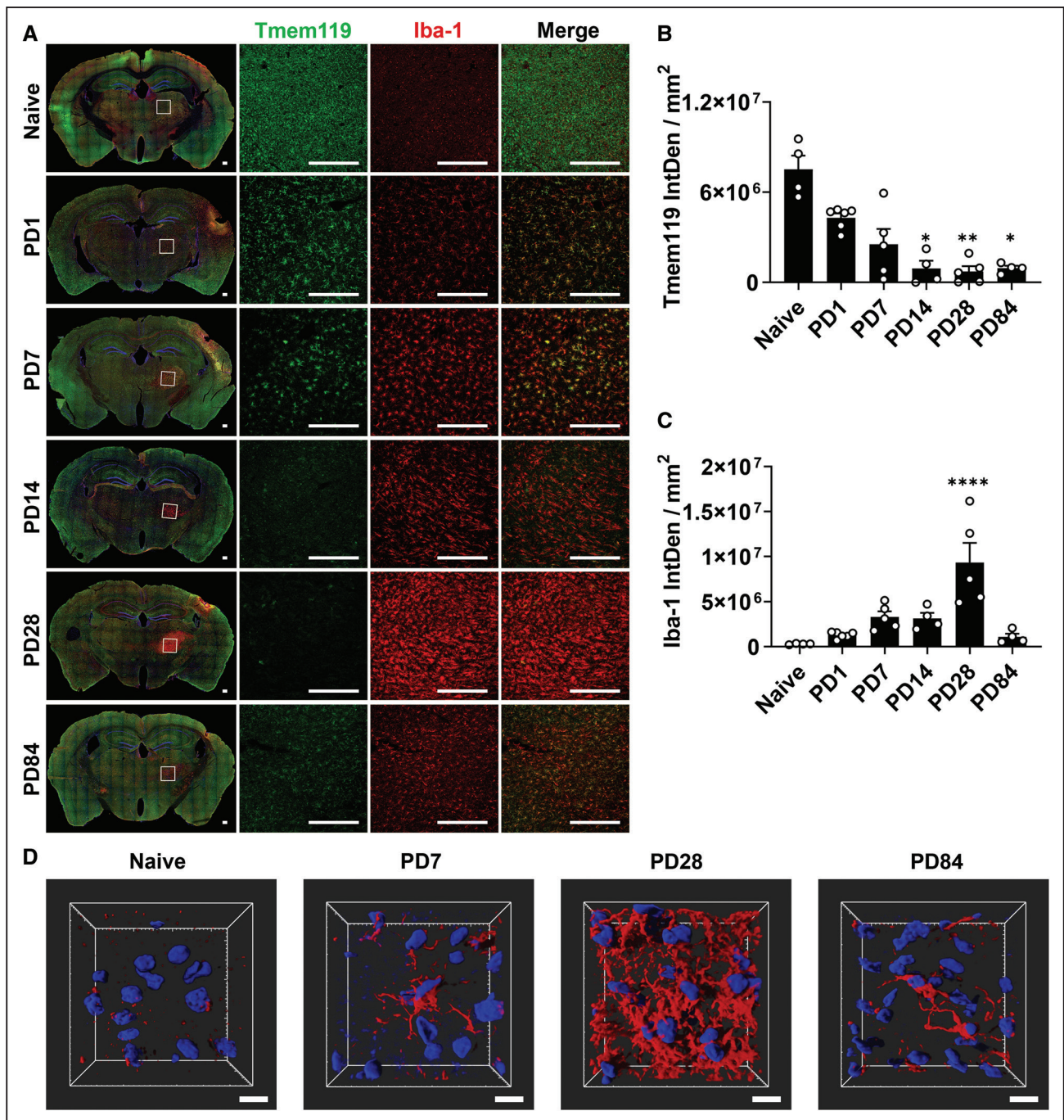


Figure 4. Microglia dynamically changed during the development of secondary thalamic injury. **A**, Representative full coronal sections show Tmem119 (transmembrane protein 119; green) and ionized calcium binding adaptor molecule 1 (Iba-1; red) immunostaining in thalamus. Enlarged images represent the square labeled region in full section images. Scale bar=250 μ m. The integrated density of Tmem119 (**B**) and the integrated density of Iba-1 (**C**) in iTH were quantified and compared with naive mice. N=4–5/time point. * P <0.05, ** P <0.01, **** P <0.0001. Data are expressed as mean \pm SEM. **D**, Representative 3-dimensional images of Iba-1 show morphology of microglia/macrophages at iTH in naive and stroke mice. Scale bar=10 μ m. PD indicates poststroke day.

thalamus after stroke (Figure 6E). Importantly, we identified a unique subtype of microglia with neurodegenerative disease-specific features. We demonstrated that a cortical stroke can robustly affect a remotely connected region such as thalamus, highlighting the importance of investigating network-wide deficits after stroke. Our findings also revealed potential cellular and molecular

targets for developing therapeutic strategies to prevent or reduce secondary thalamic injury, thereby improving recovery after stroke.

Secondary thalamic injury presented characteristics different from primary cortical injury after stroke. Neurodegeneration were delayed in the secondary injury region (iTH), in contrast to the primary injury region (iS1).

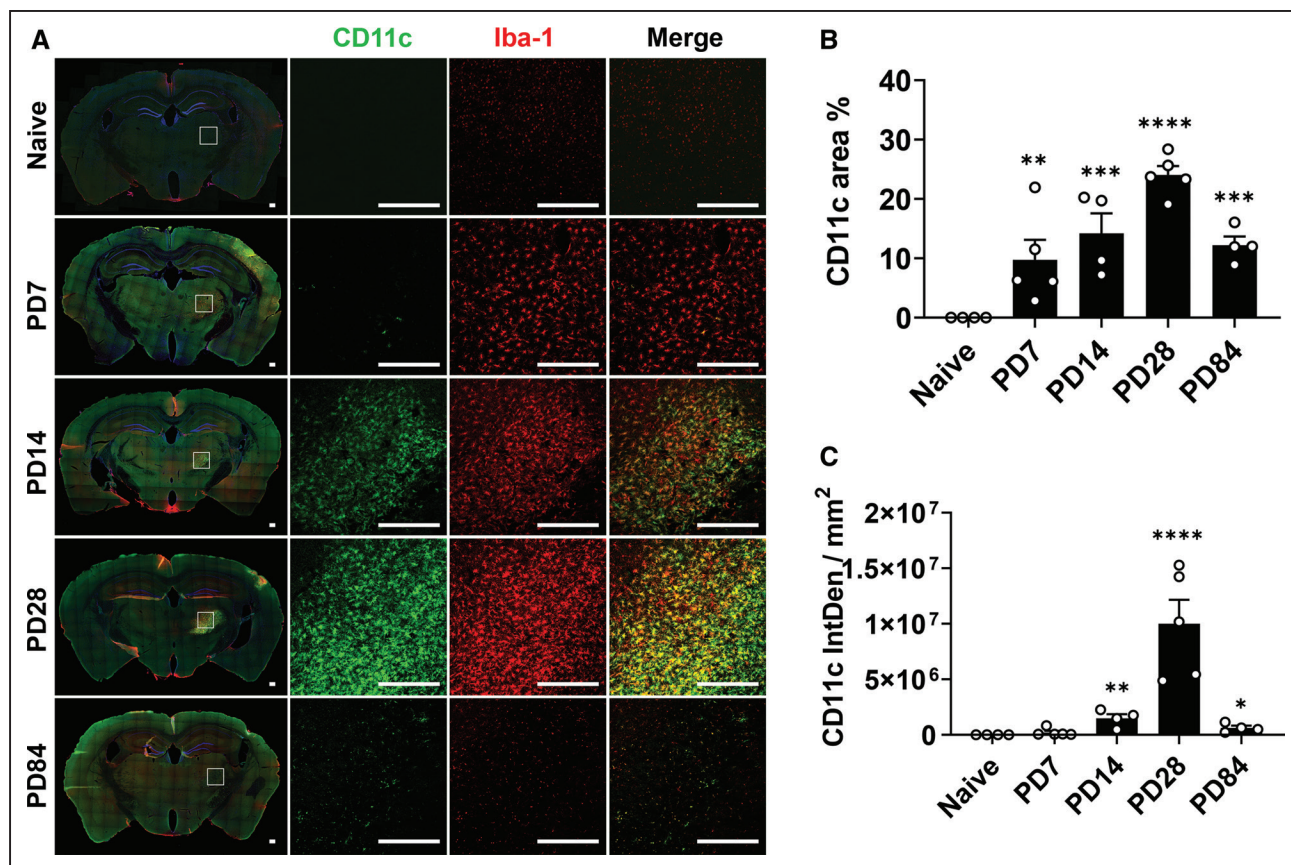


Figure 5. CD11c⁺ microglia/macrophage presented in the secondary thalamic injury.

A, Representative full coronal sections show CD11c (green) and Iba-1 (red) immunostaining in thalamus. Enlarged images represent the square labeled region in full section images. Scale bar=250 μ m. The percentage of CD11c area (**B**) and the integrated density of CD11c (**C**) were quantified in ipsilesional thalamus (iTH) and compared with naive. N=4–5/time point. * P <0.05, ** P <0.01, *** P <0.001, **** P <0.0001. Data are expressed as mean \pm SEM. PD indicates poststroke day.

Consistent with the histological findings, more transcriptome changes were observed at later time point in iTH while notable transcriptome changes in iS1 were earlier. Despite the differential transcriptome dynamics between primary and secondary injuries, neuroinflammation signaling was the top canonical pathway among other neuropathological changes in both regions and at both time points. Therefore, neuroinflammation signaling has significant implications in multiple brain regions after stroke.

Microglia are the primary resident immune cells in central nervous system mediating neuroinflammatory responses upon neuronal injury such as stroke.²⁷ Our transcriptome analysis highlighted the critical involvement of microglia in secondary thalamic injury. In contrast to previous studies,^{4,17,18,24} we specified the microglial activation in the secondary thalamic injury by immunostaining, and in conjunction with flow cytometry using multiple markers (CD45, CD11b, Ly6C, and Ly6G),^{4,17,18,28–30} we were able to differentiate microglia from other myeloid cells in the degenerative thalamus, providing specific myeloid cell type for developing immunomodulatory approaches to intervene secondary thalamic injury after stroke. Immunostaining of Tmem119 revealed a rapid microglial

activation which preceded the degeneration and neuronal loss in the remotely connected thalamus. Interestingly, we observed the Tmem119 decrease but Iba-1 increase in the degenerative thalamus. Flow-sorted CD11c⁺ studies further revealed the reduced expression of Tmem119 on CD11c⁺ microglia in the degenerative thalamus. A similar Tmem119 decrease in microglia (DAM) has been reported in other neurodegenerative diseases.²⁶

A major finding in our study was the identification and characterization of a unique subtype of microglia (CD11c⁺) in the secondary thalamic injury. We observed dynamic changes of microglia morphology and their gene expression in the thalamus after stroke, suggesting the diversity of microglia state in secondary thalamic injury. *Itgax* (CD11c) was the top significantly increased gene in the degenerative thalamus and CD11c co-expressed with the majority of Iba-1⁺ cells. CD11c is a type I transmembrane protein expressed on dendritic cells, microglia, and macrophages.²⁶ Recently, CD11c expression was found in a subtype of microglia (DAM) in models of Alzheimer disease and multiple sclerosis.^{26,31} The sorted CD11c⁺ microglia from degenerative thalamus presented common molecular signatures as DAM in neurodegenerative diseases,

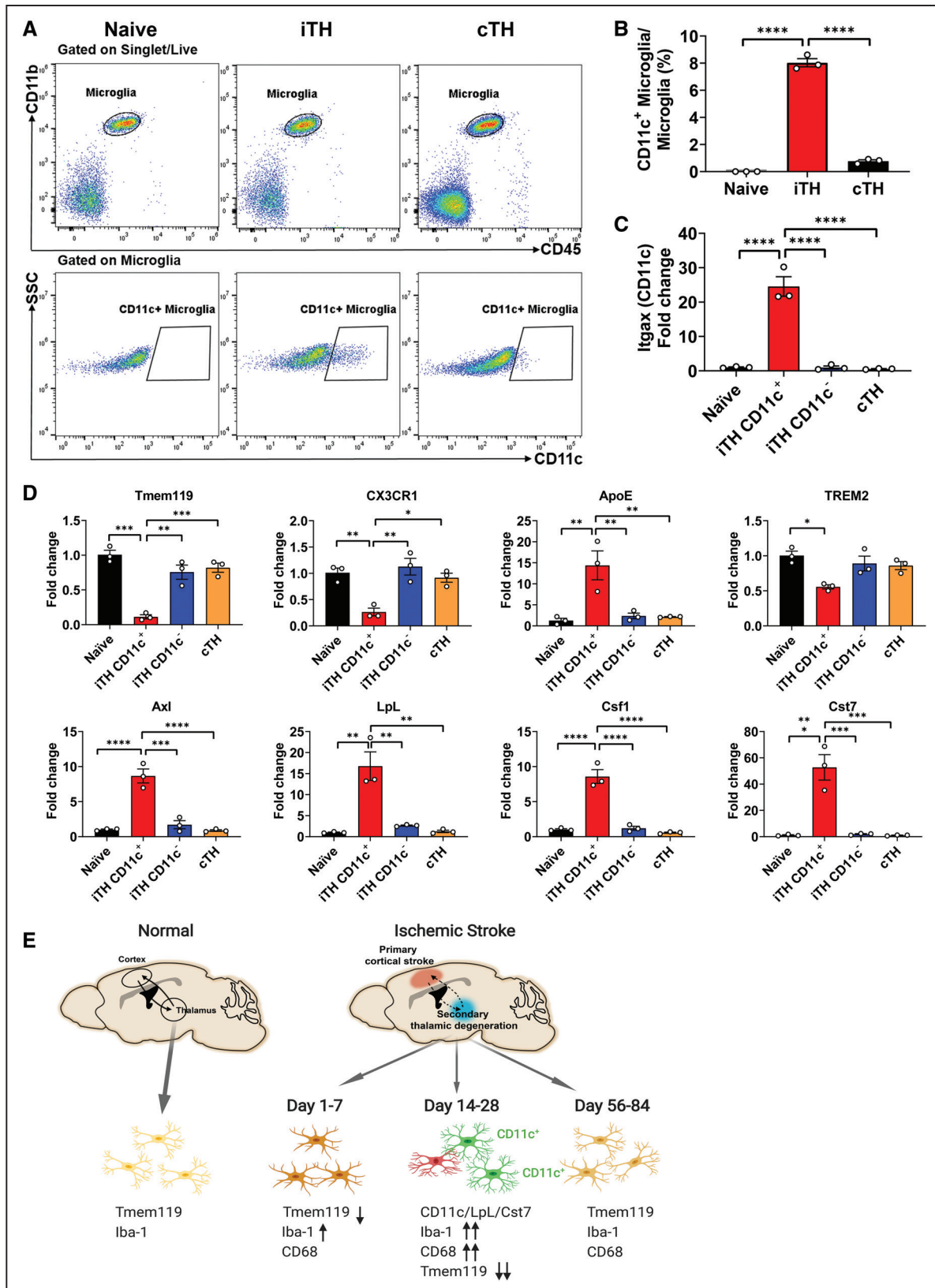


Figure 6. CD11c⁺ microglia in degenerative thalamus exhibited molecular features of disease-associated microglia (DAM).

A, Representative dot plots from FACS show gating strategy used to analyze immune cells isolated from samples of thalamus in naive, ipsilesional thalamus (iTH), and contralesional thalamus (cTH) at PD28. Microglia were gated by CD45^{int}CD11b⁺ from singlet/live cells. **B**, The percentage of CD11c⁺ microglia in naive, iTH, and cTH at PD28. **C**, The expression of *Itgax* (CD11c) was measured on iTH CD11c⁺, iTH CD11c⁻, cTH, and naive microglia. **D**, qPCR measured DAM molecular signatures (*ApoE*, *Axl*, *LpL*, *Csf1*, *Cst7*, *Tmem119*, and *CX3CR1*) on (Continued)

Figure 6 Continued. CD11c⁺ microglia from iTH, and compared with CD45^{int}CD11b⁺ microglia from naive, cTH, and CD11c⁻ microglia from iTH. N=3/group, with each sample pooled from 8 mice in PD28 group. **P*<0.05, ***P*<0.01, ****P*<0.001, *****P*<0.0001. Data are expressed in mean±SEM. **E.** Schematic figure represents the dynamics of microglia in the secondary thalamic injury. A secondary degenerative injury generates in ipsilesional thalamus after primary cortical stroke, resulting in the disruption of functional connections between cortex and thalamus. Morphological changes of microglia are shown in different shapes and colors. The key microglia-related genes are listed, and the trend of gene expression are pointed by arrowheads. A subpopulation of microglia (CD11c⁺) are present in the degenerative thalamus between PD14–28. Figure is created with BioRender.com.

suggesting that the CD11c⁺ microglia in the degenerative thalamus after stroke may be neurodegeneration-specific microglia. DAM are phagocytic cells localized with Aβ particles in Alzheimer diseases.²⁶ In addition, failure in conversion of homeostasis microglia to DAM results in cholesterol ester accumulation in brain during chronic demyelination.³² These findings suggest that DAM may play beneficial role by restricting and removing neurodegenerative damages. In our study, we observed upregulated expression of genes related to phagocytosis (Cst7) and lipid metabolism pathways (LPL and ApoE) in thalamic CD11c⁺ microglia after stroke, suggesting that CD11c⁺ microglia may be involved in phagocytosis and lipid metabolism in the secondary thalamic injury, similar to DAM in neurodegenerative diseases. Our results presented diverse status of microglia during the development of secondary thalamic injury and suggested dynamic role of microglia after stroke.

Our transcriptome analysis was limited to a coverage of 780 genes, thus we recognize that some potential pathological changes and signaling involved in secondary thalamic injury may have been missed. Future studies using high-throughput approaches are needed to further elucidate key cell types and genes involved in the degenerative thalamus. It is noteworthy to mention that the genetic changes are tightly linked to specific cell types. For example, we detected significant increase of CX3CR1 in bulk thalamus tissues after stroke. On the contrary, CX3CR1 was decreased in the sorted CD11c⁺ microglia but not in sorted CD11c⁻ microglia from the degenerative thalamus. CX3CR1 is a fractalkine receptor mainly enriched in microglia, but also expressed in astrocytes and oligodendrocytes.^{33,34} Hence, the increased CX3CR1 in bulk thalamus tissue may be due to other cell types instead of microglia. Future studies to manipulate candidate genes should selectively target specific cell types to elucidate their functional roles in secondary thalamic injury.

Clinical studies have associated secondary thalamic injury with verticality misperception after stroke³⁵ and cognitive dysfunction at 3 months after stroke.⁶ The secondary thalamic injury also independently contributes to poor functional and cognitive outcome, poststroke anxiety, and depression after focal cortical injury in patients.⁷ In addition, secondary thalamic injury offers an extended time window for therapeutic intervention. More efforts should be directed at understanding the pathological changes and mechanisms underlying secondary injuries after stroke. Our findings highlight the involvement of neuroinflammation during the development of secondary thalamic injury and revealed a panel of potential

molecular targets in neuroinflammation signaling. Our findings also identify a unique subtype of microglia as a potential cellular target, to reduce or prevent secondary thalamic injury and promote stroke recovery.

ARTICLE INFORMATION

Received August 25, 2020; final revision received October 1, 2020; accepted November 11, 2020.

Affiliations

Department of Neurosurgery (Z.C., S.S.H., T.C., A.G.F., M.Y.C., G.K.S.) and Stanford Stroke Center (Z.C., S.S.H., T.C., A.G.F., M.Y.C., G.K.S.), Stanford University School of Medicine, CA. Division of Hematology and Oncology, Department of Pediatrics, University of California, San Francisco (A.G.L.).

Acknowledgments

We thank Drs Masaki Ito and Fang Du for their assistance in magnetic resonance imaging. We also thank Drs Tonya Bliss, Marieke Cornelia Sophia Boshuizen, Yulia Zatulovskaia, Arjun Vivek Pendharkar, and Qingkun Liu for their assistance and discussion in flow cytometry/cell sorting studies. We thank Christine D. Plant for scientific editing of the article.

Sources of Funding

This work was funded by the National Institutes of Health National Institute of Neurological Disorders and Stroke R01 NS093057 award to Dr Steinberg and an American Heart Association postdoctoral fellowship 17POST33660421 to Dr Cao.

Disclosures

None.

Supplemental Materials

Supplemental Methods
Figures I–VI
Tables I–VI

REFERENCES

- Benjamin EJ, Virani SS, Callaway CW, Chamberlain AM, Chang AR, Cheng S, Chiuve SE, Cushman M, Delling FN, Deo R, et al; American Heart Association Council on Epidemiology and Prevention Statistics Committee and Stroke Statistics Subcommittee. Heart disease and stroke statistics-2018 update: a report from the American Heart Association. *Circulation*. 2018;137:e67–e492. doi: 10.1161/CIR.0000000000000558
- Seitz RJ, Azari NP, Knorr U, Binkofski F, Herzog H, Freund HJ. The role of diaschisis in stroke recovery. *Stroke*. 1999;30:1844–1850. doi: 10.1161/01.str.30.9.1844
- Iizuka H, Sakatani K, Young W. Neural damage in the rat thalamus after cortical infarcts. *Stroke*. 1990;21:790–794. doi: 10.1161/01.str.21.5.790
- Langen KJ, Salber D, Hamacher K, Stoffels G, Reifenberger G, Pauleit D, Coenen HH, Zilles K. Detection of secondary thalamic degeneration after cortical infarction using cis-4-18F-fluoro-D-proline. *J Nucl Med*. 2007;48:1482–1491. doi: 10.2967/jnumed.107.041699
- Baron JC. Mapping anterograde and retrograde degeneration after stroke. *J Neurol Neurosurg Psychiatry*. 2005;76:159–160. doi: 10.1136/jnnp.2004.051870
- Fernández-Andújar M, Doornink F, Dacosta-Aguayo R, Soriano-Raya JJ, Miralbell J, Bargalló N, López-Cancio E, Pérez de la Ossa N, Gomis M, Millán M, et al. Remote thalamic microstructural abnormalities related to cognitive function in ischemic stroke patients. *Neuropsychology*. 2014;28:984–996. doi: 10.1037/neu0000087

7. Kuchcinski G, Munsch F, Lopes R, Bigourdan A, Su J, Sagnier S, Renou P, Pruvo JP, Rutt BK, Dousset V, et al. Thalamic alterations remote to infarct appear as focal iron accumulation and impact clinical outcome. *Brain*. 2017;140:1932–1946. doi: 10.1093/brain/awx114
8. Cao Z, Balasubramanian A, Pedersen SE, Romero J, Pautler RG, Marrelli SP. TRPV1-mediated pharmacological hypothermia promotes improved functional recovery following ischemic stroke. *Sci Rep*. 2017;7:17685. doi: 10.1038/s41598-017-17548-y
9. Yu J, Li C, Ding Q, Que J, Liu K, Wang H, Liao S. Netrin-1 ameliorates blood-brain barrier impairment secondary to ischemic stroke via the activation of PI3K pathway. *Front Neurosci*. 2017;11:700. doi: 10.3389/fnins.2017.00700
10. Ross DT, Ebner FF. Thalamic retrograde degeneration following cortical injury: an excitotoxic process? *Neuroscience*. 1990;35:525–550. doi: 10.1016/0306-4522(90)90327-z
11. Liang Z, Zeng J, Liu S, Ling X, Xu A, Yu J, Ling L. A prospective study of secondary degeneration following subcortical infarction using diffusion tensor imaging. *J Neurol Neurosurg Psychiatry*. 2007;78:581–586. doi: 10.1136/jnnp.2006.099077
12. van Groen T, Puurunen K, Mäki HM, Sivenius J, Jolkonen J. Transformation of diffuse beta-amyloid precursor protein and beta-amyloid deposits to plaques in the thalamus after transient occlusion of the middle cerebral artery in rats. *Stroke*. 2005;36:1551–1556. doi: 10.1161/01.STR.0000169933.88903.cf
13. Schroeter M, Zickler P, Denhardt DT, Hartung HP, Jander S. Increased thalamic neurodegeneration following ischaemic cortical stroke in osteopontin-deficient mice. *Brain*. 2006;129(pt 6):1426–1437. doi: 10.1093/brain/awl094
14. Cao Z, Harvey SS, Bliss TM, Cheng MY, Steinberg GK. Inflammatory responses in the secondary thalamic injury after cortical ischemic stroke. *Front Neurol*. 2020;11:236. doi: 10.3389/fneur.2020.00236
15. Cheung WM, Wang CK, Kuo JS, Lin TN. Changes in the level of glial fibrillary acidic protein (GFAP) after mild and severe focal cerebral ischemia. *Chin J Physiol*. 1999;42:227–235.
16. Jones KA, Maltby S, Plank MW, Kluge M, Nilsson M, Foster PS, Walker FR. Peripheral immune cells infiltrate into sites of secondary neurodegeneration after ischemic stroke. *Brain Behav Immun*. 2018;67:299–307. doi: 10.1016/j.bbi.2017.09.006
17. Pappata S, Levasseur M, Gunn RN, Myers R, Crouzel C, Syrota A, Jones T, Kreuzberg GW, Banati RB. Thalamic microglial activation in ischemic stroke detected in vivo by PET and [¹¹C]PK1195. *Neurology*. 2000;55:1052–1054. doi: 10.1212/wnl.55.7.1052
18. Anttila JE, Albert K, Wires ES, Matlik K, Loram LC, Watkins LR, Rice KC, Wang Y, Harvey BK, Airavaara M. Post-stroke intranasal (+)-naloxone delivery reduces microglial activation and improves behavioral recovery from ischemic injury. *eNeuro*. 2018;5:ENEURO.0395-17.2018.
19. Ito M, Aswendt M, Lee AG, Ishizaka S, Cao Z, Wang EH, Levy SL, Smerin DL, McNab JA, Zeineh M, et al. RNA-sequencing analysis revealed a distinct motor cortex transcriptome in spontaneously recovered mice after stroke. *Stroke*. 2018;49:2191–2199. doi: 10.1161/STROKEAHA.118.021508
20. Hiu T, Farzampour Z, Paz JT, Wang EH, Badgely C, Olson A, Micheva KD, Wang G, Lemmens R, Tran KV, et al. Enhanced phasic GABA inhibition during the repair phase of stroke: a novel therapeutic target. *Brain*. 2016;139(pt 2):468–480. doi: 10.1093/brain/aww360
21. Paxinos G, Franklin KBJ. *Paxinos and Franklin's the Mouse Brain in Stereotaxic Coordinates*. Elsevier; 2001.
22. La Manno G, Gyllborg D, Codeluppi S, Nishimura K, Salto C, Zeisel A, Borm LE, Stott SRW, Toledo EM, Villaescusa JC, et al. Molecular diversity of midbrain development in mouse, human, and stem cells. *Cell*. 2016;167:566–580.e19. doi: 10.1016/j.cell.2016.09.027
23. Arac A, Grimbaldeston MA, Nepomuceno AR, Olayiwola O, Pereira MP, Nishiyama Y, Tsykin A, Goodall GJ, Schlecht U, Vogel H, et al. Evidence that meningeal mast cells can worsen stroke pathology in mice. *Am J Pathol*. 2014;184:2493–2504. doi: 10.1016/j.ajpath.2014.06.003
24. Zhang Y, Chen K, Sloan SA, Bennett ML, Scholze AR, O'Keefe S, Phatnani HP, Guarnieri P, Caneda C, Ruderisch N, et al. An RNA-sequencing transcriptome and splicing database of glia, neurons, and vascular cells of the cerebral cortex. *J Neurosci*. 2014;34:11929–11947. doi: 10.1523/JNEUROSCI.1860-14.2014
25. Bennett ML, Bennett FC, Liddel SA, Ajami B, Zamanian JL, Fernhoff NB, Mulinuway SB, Bohlen CJ, Adil A, Tucker A, et al. New tools for studying microglia in the mouse and human CNS. *Proc Natl Acad Sci U S A*. 2016;113:E1738–E1746. doi: 10.1073/pnas.1525528113
26. Keren-Shaul H, Spinrad A, Weiner A, Matcovitch-Natan O, Dvir-Szternfeld R, Ulland TK, David E, Baruch K, Lara-Astaiso D, Toth B, et al. A unique microglia type associated with restricting development of Alzheimer's disease. *Cell*. 2017;169:1276–1290.e17. doi: 10.1016/j.cell.2017.05.018
27. Rayasam A, Hsu M, Kijak JA, Kissel L, Hernandez G, Sandor M, Fabry Z. Immune responses in stroke: how the immune system contributes to damage and healing after stroke and how this knowledge could be translated to better cures? *Immunology*. 2018;154:363–376. doi: 10.1111/imm.12918
28. Ritzel RM, Patel AR, Grenier JM, Crapser J, Verma R, Jellison ER, McCullough LD. Functional differences between microglia and monocytes after ischemic stroke. *J Neuroinflammation*. 2015;12:106. doi: 10.1186/s12974-015-0329-1
29. Liu Q, Johnson EM, Lam RK, Wang Q, Bo Ye H, Wilson EN, Minhas PS, Liu L, Swarovski MS, Tran S, et al. Peripheral TREM1 responses to brain and intestinal immunogens amplify stroke severity. *Nat Immunol*. 2019;20:1023–1034. doi: 10.1038/s41590-019-0421-2
30. Jones KA, Zoukir I, Patience M, Clarkson AN, Isgaard J, Johnson SJ, Spratt N, Nilsson M, Walker FR. Chronic stress exacerbates neuronal loss associated with secondary neurodegeneration and suppresses microglial-like cells following focal motor cortex ischemia in the mouse. *Brain Behav Immun*. 2015;48:57–67. doi: 10.1016/j.bbi.2015.02.014
31. Deczkowska A, Keren-Shaul H, Weiner A, Colonna M, Schwartz M, Amit I. Disease-associated microglia: a universal immune sensor of neurodegeneration. *Cell*. 2018;173:1073–1081. doi: 10.1016/j.cell.2018.05.003
32. Nugent AA, Lin K, van Lengerich B, Lianoglou S, Przybyla L, Davis SS, Llapashtica C, Wang J, Kim DJ, Xia D, et al. TREM2 regulates microglial cholesterol metabolism upon chronic phagocytic challenge. *Neuron*. 2020;105:837–854.e9. doi: 10.1016/j.neuron.2019.12.007
33. Hammond TR, Dufort C, Dissing-Olesen L, Giera S, Young A, Wysoker A, Walker AJ, Gergits F, Segel M, Nemesh J, et al. Single-cell rna sequencing of microglia throughout the mouse lifespan and in the injured brain reveals complex cell-state changes. *Immunity*. 2019;50:253–271 e256.
34. Sunnemark D, Eltayeb S, Nilsson M, Wallström E, Lassmann H, Olsson T, Berg AL, Ericsson-Dahlstrand A. CX3CL1 (fractalkine) and CX3CR1 expression in myelin oligodendrocyte glycoprotein-induced experimental autoimmune encephalomyelitis: kinetics and cellular origin. *J Neuroinflammation*. 2005;2:17. doi: 10.1186/1742-2094-2-17
35. Santos TEG, Baggio JAO, Rondinoni C, Machado L, Weber KT, Stefano LH, Santos AC, Pontes-Neto OM, Leite JP, Edwards DJ. Fractional anisotropy of thalamic nuclei is associated with verticality misperception after extra-thalamic stroke. *Front Neurol*. 2019;10:697. doi: 10.3389/fneur.2019.00697